NOVATEUR PUBLICATIONS
INTERNATIONAL JOURNAL OF INNOVATIONS IN ENGINEERING RESEARCH AND TECHNOLOGY [IJIERT]
ISSN: 2394-3696
VOLUME 4, ISSUE 4, Apr.-2017

SYNTHESIS OF POWER PROCESSING IN DC DISTRIBUTION SYSTEMS USING CASCADED CONVERTERS, LFRS AND SLIDING-MODE CONTROL TECHNIQUE.

INGLE S.V.
PG Department, M.B.E'S.C.O.E/B.A.M.U, India, soniyaingle1992@gmail.com

S .S. SANKESHWARI
*PG Department, M.B.E'S.C.O.E/B.A.M.U, India, * sankeswaril@gmail.com*

ABSTRACT
Switching dc-dc converters are widely used to interface the dc output of renewable energy resources with power distribution systems in order to facilitate the use of energy at the customer side. In this paper, a system connected to a PV panel, fuel cell ,wind turbine consisting of two cascaded dc-dc boost converters under sliding-mode control and working as loss-free resistors , gyrator ,transformer is studied. The modeling, simulation, and design of the system are addressed. First, an ideal reduced-order sliding-mode dynamics model is derived from the full-order switched model taking into account the sliding constraints, the nonlinear characteristic of the PV module, and the dynamics of the MPPT controller. For this model, a design-oriented averaged model is obtained and its dynamic behavior is analyzed showing that the system is asymptotically globally stable. Moreover, the proposed system can achieve a high conversion ratio with an efficiency close to 95% for a wide range of working power. Numerical simulations and experimental results corroborate the theoretical analysis and illustrate the advantages of this architecture in PV systems. The proposed method can be used for the other DC/DC converter. This paper proposes the new cascaded series parallel design for improved dynamic performance of DC-DC buck boost converters by a new Sliding Mode Control (SMC) method. The converter is controlled using Sliding Mode Control method that utilizes the converter's duty ratio to determine the skidding surface. System modeling and simulation results are presented. Microgrid is one of new conceptual power systems for smooth installation of many distributed generations (DGs). While most of the microgrids adopt ac distribution as well as conventional power systems, dc microgrids are proposed and researched for the good connection with dc output type sources such as photovoltaics (PV), fuel cell, and secondary battery. Moreover, if loads in the system are supplied with dc power, the conversion losses from sources to loads are reduced compared with ac microgrid. As one of the dc microgrids, we propose "low voltage bipolar type dc microgrid" which can supply super high quality power with 3-wire dc distribution line.

INTRODUCTION
Clean renewable energy resources have been given increasing interest in recent years, due to concerns about global warming and its related harmful greenhouse effect, air quality, and sustainable development . In the future power grid, not only the utilities, but also the users can produce electric energy by aggregating distributed generation sources . In that context, photovoltaic (PV) arrays, wind turbines, and batteries are used to feed a main (dc or ac) bus connected to its loads, as well as the utility grid, forming the so-called nano grid system [2] . Nano grids can then work in the stand-alone mode or they can be connected to the utility grid performing peak shaving and smooth transitions between the different modes of operation.
Modern electronic systems require high-quality, small, lightweight, reliable, and efficient power supplies. So, the DC/DC converters are widely used in many industrial and electrical systems. The most familiar are switching power supplies, DC drives, and photovoltaic systems. The stability is an important aspect in the design of switch mode power supplies; a feedback control is used to achieve the required performance. Ideally the circuit is in steady state, but actually the circuit is affected by line and load variations (disturbances), as well as variation of the circuit component (robustness). These parameters have a severe effect on the behavior of switch mode power supply and may cause instability. Design of controller for these converters is a major concern in power converters design [1–4] Sliding mode control is a well-known discontinuous feedback control technique which has been exhaustively explored in many books and journal articles. The technique is naturally suited for the regulation of switched controlled systems, such as power

electronics devices, in general, and DC/DC power converters, in particular . Many sliding mode controllers have been proposed and used for DC/DC converters . These controllers are direct or indirect control method . The direct method is proposed in. In, the output capacitor current of DC/DC converter is used to control the output voltage. The differences of the DC/DC output voltage and the reference voltage enter the proportional-Integrator (PI) type controller, and then the output capacitor current of DC/DC converter is decreased from the output of controller . The output voltage and inductor current are used to control of DC/DC converter in . These references have not completely investigated the load and line as well as reference regulations.[4]

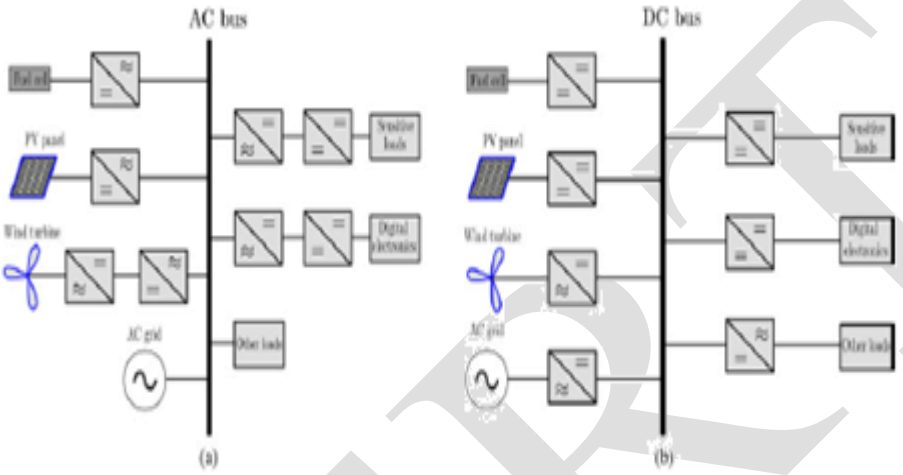

Fig.1 (a) an ac distribution system (b) a dc distribution system

DC/DC CONVERTERS

The DC-DC converters can be divided into two main types: (1) hard-switching pulse width modulated (PWM) converters and (2) resonant and soft-switching converters [1].Advantages of PWM converters include low component count, high efficiency, constant frequency operation, relatively simple control and commercial availability of integrated circuit controllers, and ability to achieve high conversion ratios for both step-down and step-up applications. The block diagram of the DC/DC converter is shown in Figure 1. It is well known that if many DGs are installed into a utility grid, they can cause problems such as voltage rise and protection problem. To solve these problems, new conceptual electric power systems were proposed. As one of the concepts, micro grids are especially researched all over the world.[7]

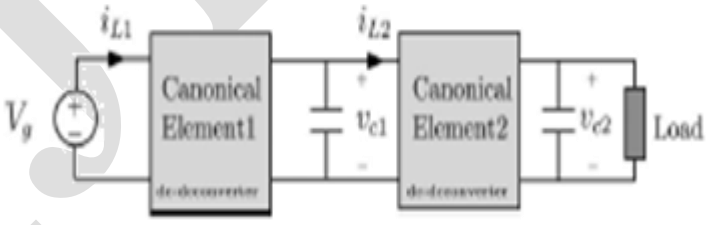

Fig. 2 dc – dc converter

Canonical elements have been used in different contexts and applications over the past two decades. The two majors axes of application of the canonical elements concept are as follows: first, the implementation of a specific function in energy processing such as power factor correction (PFC), voltage regulation, and impedance matching . The second refers to the use of these elements in modelling dynamical systems, power processing systems, and electric drives [1]. Although other techniques of implementation exist a well-known method for realization of the above canonical elements is the induction of certain sliding motions in appropriate converters [2].Fig. 3 shows the ideal block diagram of a generalized canonical element for power processing consisting of a switching converter which is controlled by means of a sliding-mode regulation loop.

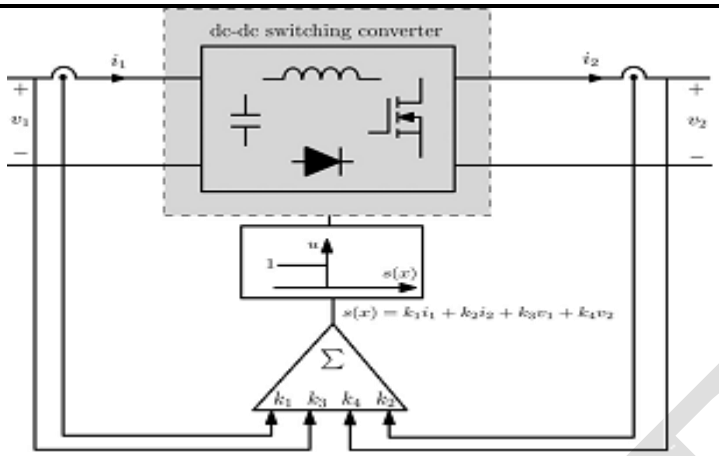

Fig. 3 shows the ideal block diagram of a generalized canonical element for power processing

The general switching function can be expressed by

$$s(x) = k_1 i_1 + k_2 i_2 + k_3 v_1 + k_4 v_2. \tag{1}$$

As an example, the goal of the synthesis of a dc transformer is to design a switching structure whose input and output variables in the steady state are related according to the following equation:

$$V_2 = nV_1 \text{ and } I_1 = nI_2 \tag{2}$$

Similarly, the synthesis of a power gyrator requires a switching structure leading to the following set of relations between the steady-state input and output variables

$$\text{g-gyrator type } I_2 = gV_1, \quad I_1 = gV_2 \tag{3}$$

$$\text{r-gyrator type } V_1 = rI_2, \quad V_2 = rI_1 \tag{4}$$

Llly LFR

$$V_1 = rI_1 \text{ and } V_1 I_1 = V_2 I_2. \tag{5}$$

1. DC TRANSFORMER

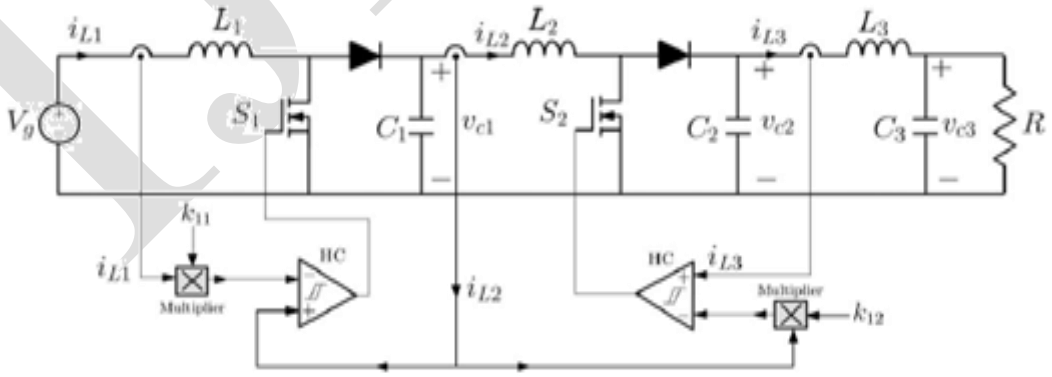

Fig. 4 Schematic diagram for two cascaded boost-based dc transformers by using SMC

In this study, the cascade connection of two canonical elements based on the BOF converter is used to obtain a voltage conversion ratio around 25. These canonical elements have been synthesized by means of a sliding-mode regulation loop. The SMC is usually implemented by using a hysteretic comparator (HC). It is

worth noting that the existence of this HC will result in a self-oscillating system with a variable switching frequency which will depend mainly on the hysteresis width h and the operating point. The considered parameters of the BOF converter

- **CASCADE CONNECTION OF TWO BOOST-BASED DC TRANSFORMERS**

A. SYSTEM DESCRIPTION

The cascade connection of two dc transformers based on the BOF converter under SMC.

$$V_{C3} = nV_g \text{ and } I_{L1} = nI_{L3}. \tag{6}$$

B. FULL-ORDER SWITCHED MODEL

The cascade connection of two BOF converters can be represented by the following set of differential equations:

$$\frac{di_{L1}}{dt} = \frac{V_g}{L_1} - \frac{(1-u_1)v_{c1}}{L_1} \tag{7}$$

$$\frac{di_{L2}}{dt} = \frac{v_{c1}}{L_2} - \frac{(1-u_2)v_{c2}}{L_2} \tag{8}$$

$$\frac{di_{L3}}{dt} = \frac{v_{c2}}{L_3} - \frac{v_{c3}}{L_3} \tag{9}$$

$$\frac{dv_{c1}}{dt} = \frac{(1-u_1)i_{L1}}{C_1} - \frac{i_{L2}}{C_1} \tag{10}$$

$$\frac{dv_{c2}}{dt} = \frac{(1-u_2)i_{L2}}{C_2} - \frac{i_{L3}}{C_2} \tag{11}$$

$$\frac{dv_{c3}}{dt} = \frac{i_{L3}}{C_3} - \frac{v_{c3}}{RC_3} \tag{12}$$

All the parameters that appear in (7)–(12) are shown in Fig. 4

C. EQUIVALENT CONTROL

SMC can be classified as an order reduction control, and ideally, the trajectories of the switched system are maintained on the switching boundary where the dynamics can be described by a reduced-order dynamical model. These equivalent control variables can be obtained by imposing that the trajectories are evolving on the switching manifolds.

$$\dot{s}_1(x) = \frac{di_{L2}}{dt} - k_{11}\frac{di_{L1}}{dt} = 0 \tag{13}$$

$$\dot{s}_2(x) = \frac{di_{L3}}{dt} - k_{12}\frac{di_{L2}}{dt} = 0. \tag{14}$$

From (7)–(12) and (13)–(14), the following expressions are obtained for the equivalent control variables ueq1 (x) and ueq2(x)

$$u_{\mathrm{eq1}}(x) = 1 - \frac{1}{v_{c1}}(\alpha_1(v_{c3} - v_{c2}) - V_g) \tag{15}$$

$$u_{eq2}(x) = 1 - \frac{1}{v_{c2}}(\alpha_2(v_{c3} - v_{c2}) - v_{c1})$$

(16)

where α1 = L1/(L3k11k12) and α2 = L2/(L3k12).

D. IDEAL SLIDING DYNAMICS AND SLIDING-MODE CONDITIONS

The following reduced-order ideal sliding dynamics is obtained

$$\frac{di_{L1}}{dt} = \frac{2V_g}{L_1} - \frac{v_{c3} - v_{c2}}{k_{11}^2 L_3}$$

(17)

$$\frac{dv_{c1}}{dt} = \left(\frac{1}{v_{c1}}\left(\frac{\alpha_1 k_{12}}{k_{11}}(v_{c3} - v_{c2}) + V_g\right) - k_{11}\right)\frac{i_{L1}}{C_1}$$

(18)

$$\frac{dv_{c2}}{dt} = \left(\frac{\alpha_2 k_{12}}{k_{11}^2 v_{c2}}(v_{c3} - v_{c2}) + \frac{k_{11} v_{c1}}{v_{c2}} - k_{11}k_{12}\right)\frac{i_{L1}}{C_2}$$

(19)

$$\frac{dv_{c3}}{dt} = \frac{k_{11}k_{12}i_{L1}}{C_3} - \frac{v_{c3}}{RC_3}.$$

(20)

The equilibrium point can be obtained by forcing the time derivative of the ideal sliding dynamics state variables to be null. From (17)–(20), the equilibrium point of the ideal sliding dynamics is given by

$$x^* = [I_{L1}, V_{c1}, V_{c2}, V_{c3}]^\top = \left[\frac{V_g}{k^2 R}, \frac{V_g}{k_{11}}, \frac{V_g}{k}, \frac{V_g}{k}\right]^\top$$

(21)

These steady-state equivalent controls can be expressed as follows:

$$U_{eq1} = 1 - k_{11} \text{ and } U_{eq2} = 1 - k_{12}.$$

(22)

E. STABILITY ANALYSIS OF THE IDIAL SLIDING MODE DYNAMIC MODEL.

The stability of the linearized system can be studied by using the Jacobian matrix **J** corresponding to (17)–(20) and evaluating it at the equilibrium point x∗ given in (21). This matrix can be expressed as follows:

$$\mathbf{J} = \begin{pmatrix} 0 & 0 & \frac{1}{kL_3} & -\frac{1}{kL_3} \\ 0 & \frac{-1}{k_{12}^2 RC_1} & \frac{-\alpha_1}{kk_{12}RC_1} & \frac{\alpha_1}{kk_{12}RC_1} \\ 0 & \frac{1}{k_{12}RC_2} & -\frac{\alpha_2}{k_{12}RC_2} - \frac{1}{RC_2} & \frac{\alpha_2}{k_{12}RC_2} \\ \frac{k}{C_3} & 0 & 0 & -\frac{1}{RC_3} \end{pmatrix}$$

(23)

The characteristic polynomial of the linearized system is pJ (s) = det(**J** − s**I**), where **I** is the unitary matrix which can be written in the following form:

$$p_J(s) = s^4 + a_1 s^3 + a_2 s^2 + a_3 s + a_4.$$

(24)

SIIMULATION RESULT:

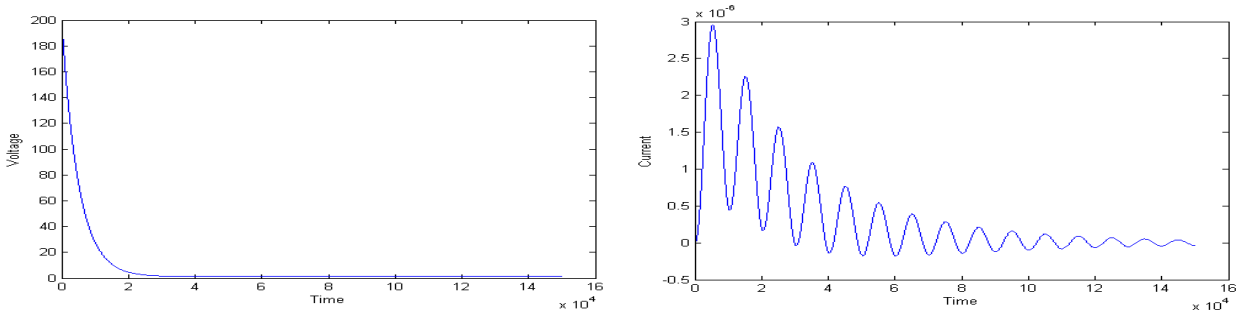

a) Voltage **b) Current**

Fig.5 Waveform Of Two boost-based dc Transformers without SMC A) Voltage and Current

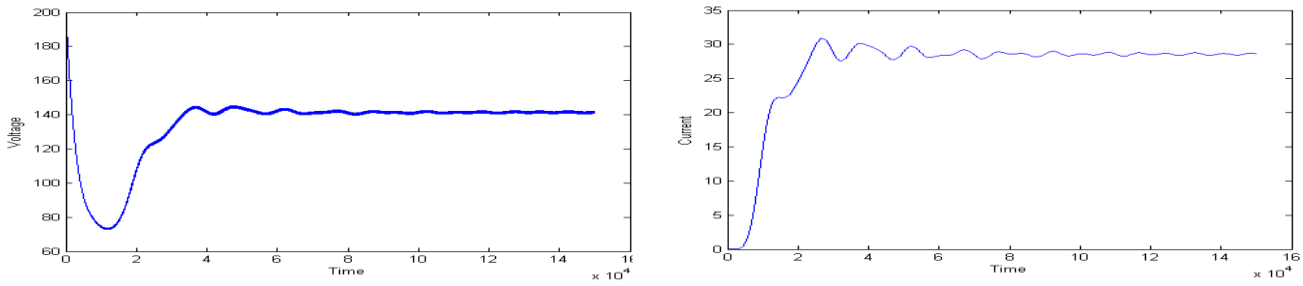

a) Voltage **b)Current**

Fig.6 Waveform Of Two boost-based dc Transformers by using SMC A) Voltage and Current

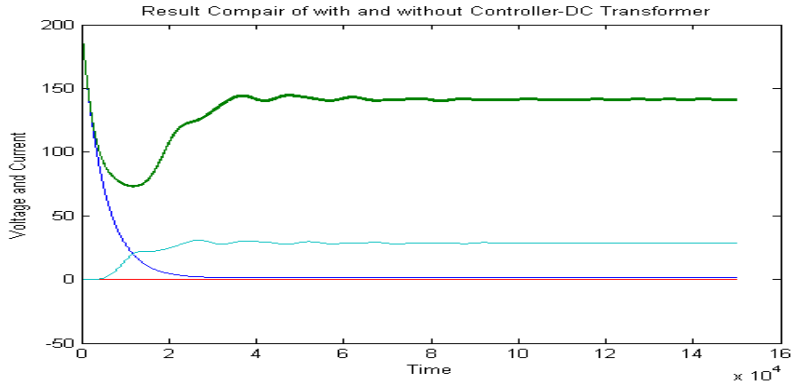

Fig.7 Waveform Of Two boost-based dc Transformers by using SMC and without SMC

2. G- GYRATORS

The same study in the previous section is carried out for two cascaded boost converters acting as g-gyrators with controlled input current.

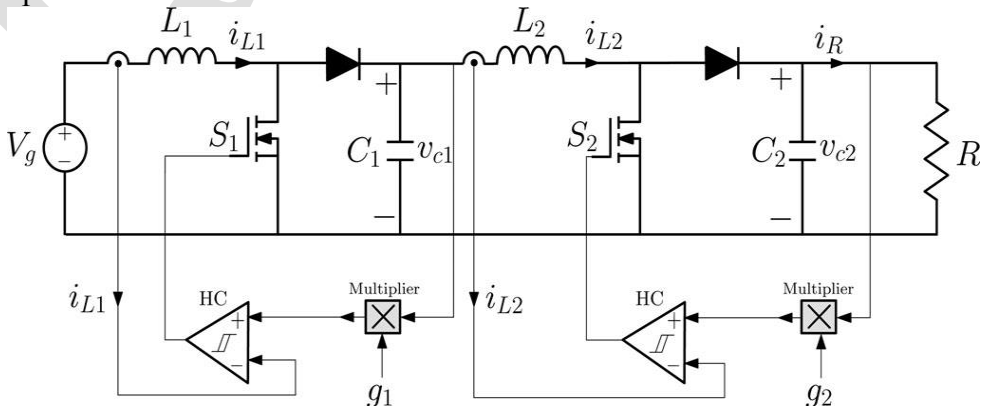

Fig. 8. Schematic diagram for two cascaded boost-based g-gyrators by imposing SMC.

- **CASCADE CONNECTION OF TWO BOOST-BASED G-GYRATORS**

A) SYSTEM DESCRIPTION

Combining the steady-state expressions of both gyrators, the following relationship is obtained:

$$V_{c2} = \frac{g_1}{g_2} V_g \text{ and } I_R = \frac{g_2}{g_1} I_{L1}.$$

(25)

B) FULL-ORDER SWITCHED MODEL

Considering that both converters operate in CCM, the cascade connection of two boost based gyrators of Fig.can be represented by the following set of differential equations:

$$\frac{di_{L1}}{dt} = \frac{V_g}{L_1} - \frac{v_{c1}}{L_1}(1 - u_1)$$

(26)

$$\frac{di_{L2}}{dt} = \frac{v_{c1}}{L_2} - \frac{v_{c2}}{L_2}(1 - u_2)$$

(27)

$$\frac{dv_{c2}}{dt} = \frac{i_{L2}}{C_2}(1 - u_2) - \frac{v_{c2}}{RC_2}.$$

(28)

$$\frac{dv_{c1}}{dt} = \frac{i_{L1}}{C_1}(1 - u_1) - \frac{i_{L2}}{C_1}$$

(29)

C) EQUIVALENT CONTROL

Following the same procedure used for the dc transformer, the equivalent control variables ueq1 and ueq2 can be obtained.Their expressions are given by

$$u_{eq1} = 1 - \frac{1}{v_{c1}}(\beta_1 V_g + \beta_2 v_{c2})$$

(30)

$$u_{eq2} = 1 - \beta_3 \frac{v_{c1}}{v_{c2}} - \beta_4$$

(31)

where β1 = C1/(g21L1 + C1), β2 = gL1/(g21L1 + C1), g =g1g2, β3 = C2/(g22L2 + C2) and β4 = g2L2/(R(g22L2 +C2)).Constrained on the sliding manifold, the motion of the system is described by the following reduced-order ideal sliding-mode dynamics model:

$$\frac{dv_{c1}}{dt} = \frac{g_1 V_g}{g_1^2 L_1 + C_1} + (\beta_2 g_1 - g_2)\frac{v_{c2}}{C_1}$$

(32)

$$\frac{dv_{c2}}{dt} = \frac{g_2 v_{c1}}{g_2^2 L_2 + C_2} + (\beta_4 g_2 - 1)\frac{v_{c2}}{RC_2}.$$

(33)

The coordinates of the equilibrium point are given by

$$x^* = [V_{c1}, V_{c2}]^\top = [\frac{g_1}{g_2^2 R} V_g, \frac{g_1}{g_2} V_g]^\top.$$

(34)

D) SLIDING-MODE CONDITIONS

The equivalent control variables at the equilibrium point can be obtained by substituting (34) into (30) and (31). In the steady state, these control variables are given by

$$U_{\text{eq1}} = 1 - \frac{g_2^2 R}{g_1} \text{ and } U_{\text{eq2}} = 1 - \frac{1}{g_2 R}.$$

(35)

It can be observed that this condition depends on the load resistance and under load change, the sliding motion can be lost.

$$\frac{1}{g_2} < R < \frac{g_1}{g_2^2}.$$

(36)

E) Stability Analysis of the Ideal Sliding Dynamics Model

In the case of the gyrator, the characteristic polynomial equation is given by the following expression:

$$s^2 + \frac{\beta_4}{g_2 L_2} s + \frac{\beta_1 \beta_3 g_2^2}{C_1 C_2} = 0$$

(37)

Which is a second-order equation and has two complex conjugates poles in the left half-plane and the system is unconditionally stable. By including the additional LC filter at the output of the second converter, the characteristic equation will be fourth order and the system stability will not be altered. In applications in which a pulsating output current is not allowed, the most suitable option will be the inclusion of the LC output filter.

SIMULATION RESULT

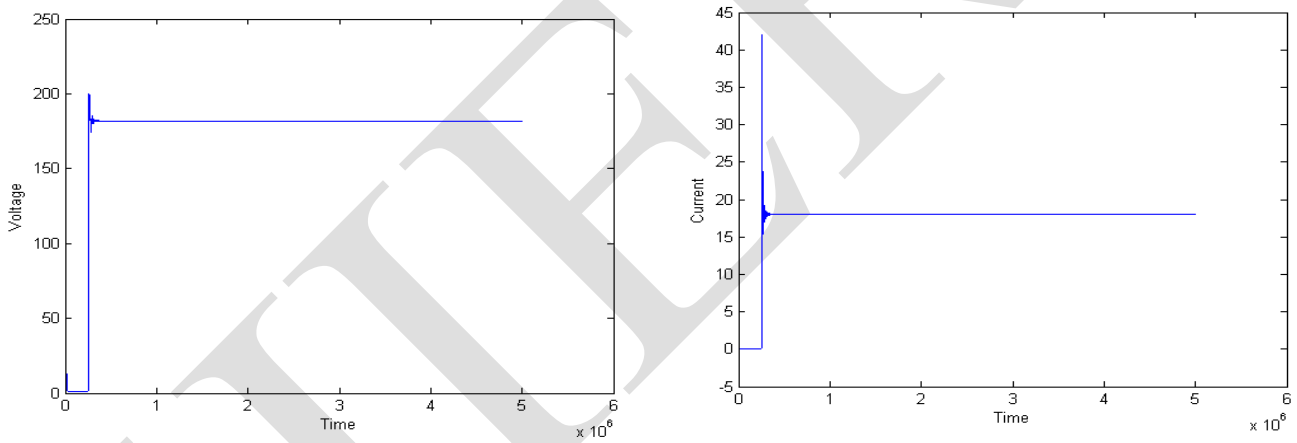

A) Voltage **B) Current**

Fig. 9 Waveform Of Two boost-based gyrator Without SMC A)Voltage and B) Current

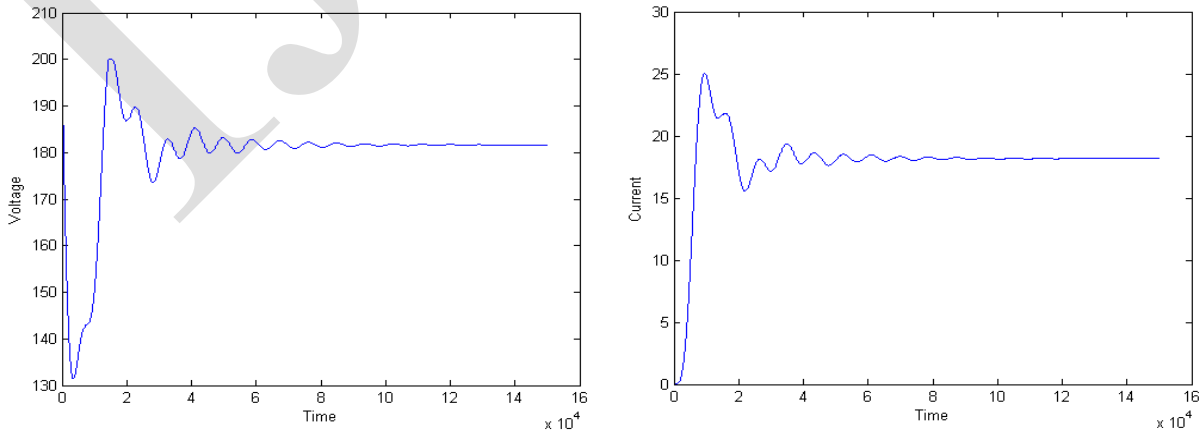

A) Voltage **B) Current**

Fig. 10 Waveform Of Two boost-based gyrator by using SMC A)Voltage and B) Current

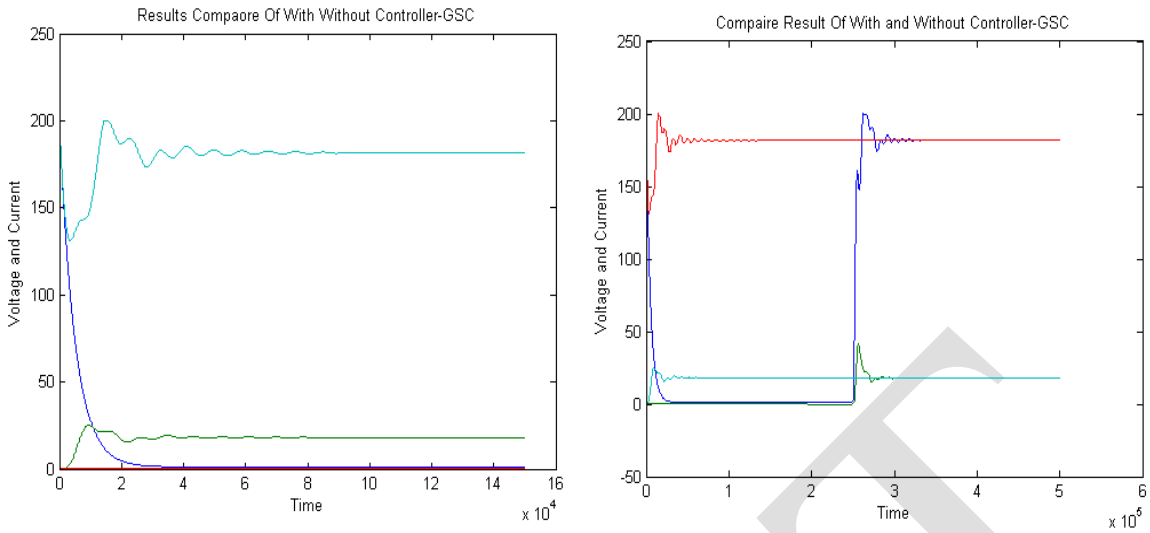

Fig. 11 Waveform Of Two boost-based gyrator by using SMC and without SMC

3. LFRS

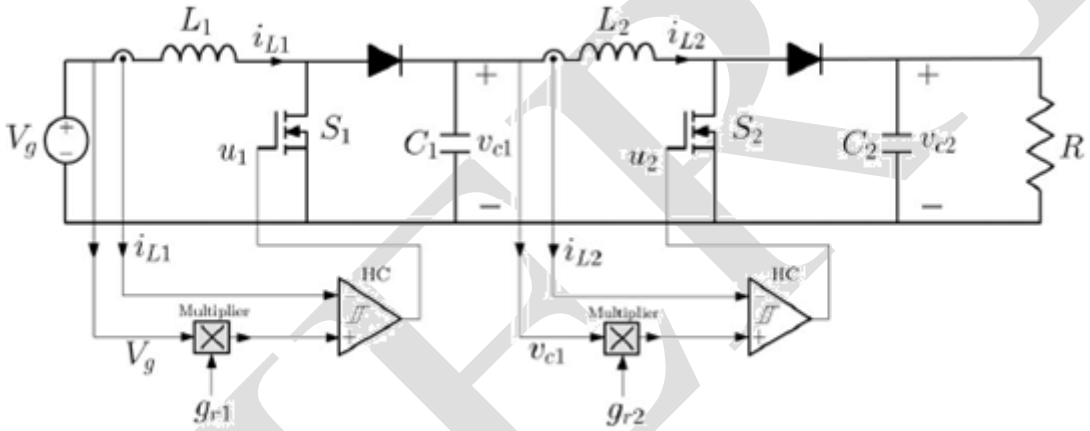

Fig. 12. Schematic diagram for two cascaded boost-based LFRs by using SMC.

- **CASCADE CONNECTION OF TWO BOOST-BASED LFRS**

A. SYSTEM DESCRIPTION

$$V_{c1} = V_g\sqrt{\frac{g_{r1}}{g_{r2}}} \text{ and } V_{c2} = V_g\sqrt{Rg_{r1}}.$$

(38)

The output voltage depends on three parameters: the input voltage Vg , the conductance gr1 of the first LFR, and the load resistance R. Furthermore, the intermediatevoltage Vc1 depends on the conductances gr1, gr2 of both LFR and the input voltage. Therefore, in a potential application of this structure, the conductance of the first LFR could be used voltage Vc1 .[3]

B. EQUIVALENT CONTROL

Using the same procedure of the previous sections.

$$u_{eq1} = 1 - \frac{V_g}{v_{c1}}$$

(39)

$$u_{eq2} = 1 - \gamma_1\frac{v_{c1}}{v_{c2}} + \gamma_2\frac{V_g^2}{v_{c1}v_{c2}}$$

(40)

where γ1 = (C1 + g2r2L2)/C1 and γ2 = gr1gr2L2/C1.

In this case, the sliding-mode regime will exist provided that Vg < vc1 < vc1L , where the critical value vc1L is given by

$$v_{c1L} = \frac{v_{c2}}{2\gamma_1} + \sqrt{\frac{v_{c2}^2}{4\gamma_1^2} + \frac{V_g^2\gamma_2}{\gamma_1}}.$$

(41)

the following model for ideal sliding dynamics is obtained:

$$\frac{dv_{c1}}{dt} = \frac{V_g}{v_{c1}}\frac{i_{L1}}{C_1} - \frac{i_{L2}}{C_1}$$

(42)

$$\frac{dv_{c2}}{dt} = \frac{i_{L2}}{C_2}\left(\gamma_1\frac{v_{c1}}{v_{c2}} - \gamma_2\frac{V_g^2}{v_{c1}v_{c2}}\right) - \frac{v_{c2}}{RC_2}.$$

(43)

The equilibrium point corresponding to (42)and(43) is given by

$$x^* = [V_{c1}, V_{c2}]^\top = [V_g\sqrt{\frac{g_{r1}}{g_{r2}}}, V_g\sqrt{Rg_{r1}}]^\top.$$

(44)

C. SLIDING-MODE CONDITIONS

The equivalent control variables at the equilibrium point can be obtained (44) into (39) and (40) to obtain the following equations:

$$U_{eq1} = 1 - \sqrt{\frac{g_{r2}}{g_{r1}}} \text{ and } U_{eq2} = 1 - \frac{1}{\sqrt{Rg_{r2}}}.$$

(45)

D. STABILITY ANALYSIS OF THE IDEAL SLIDING DYNAMICS MODEL.

The characteristic polynomial equation is obtained by linearizing (42) and (43) around the equilibrium point given in (44). This polynomial equation can be expressed as follows:

$$(s + \frac{2g_{r2}}{C_1})(s + \frac{2}{RC_2}) = 0.$$

(46)

SIMULATION RESULT

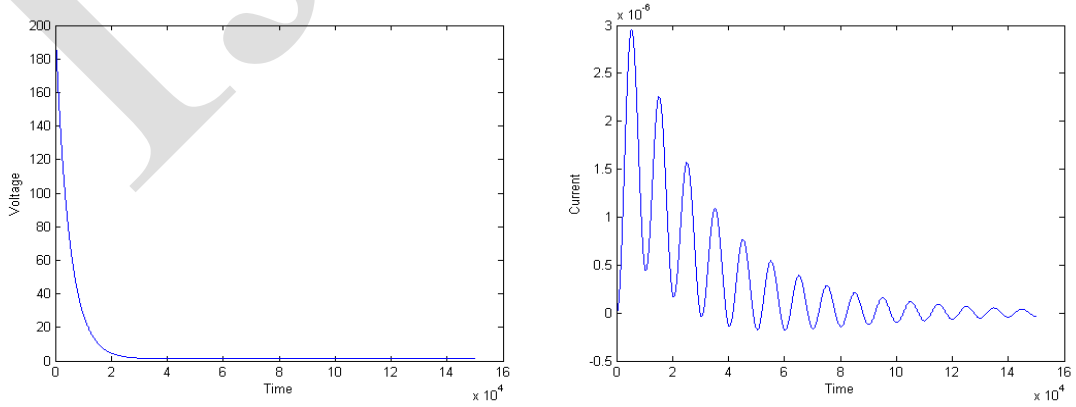

A) Voltage **B)Current**

Fig.13 Waveform Of Two boost-based LFR Without SMC A) Voltage and B) Current

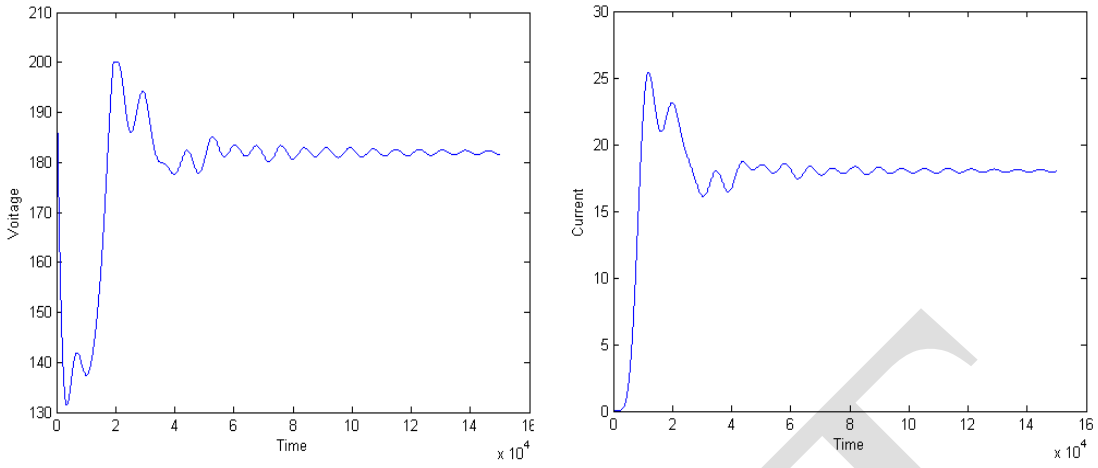

A) Voltage **B) Current**

Fig. 14 Waveform Of Two boost-based LFR by using SMC A) Voltage and B) Current

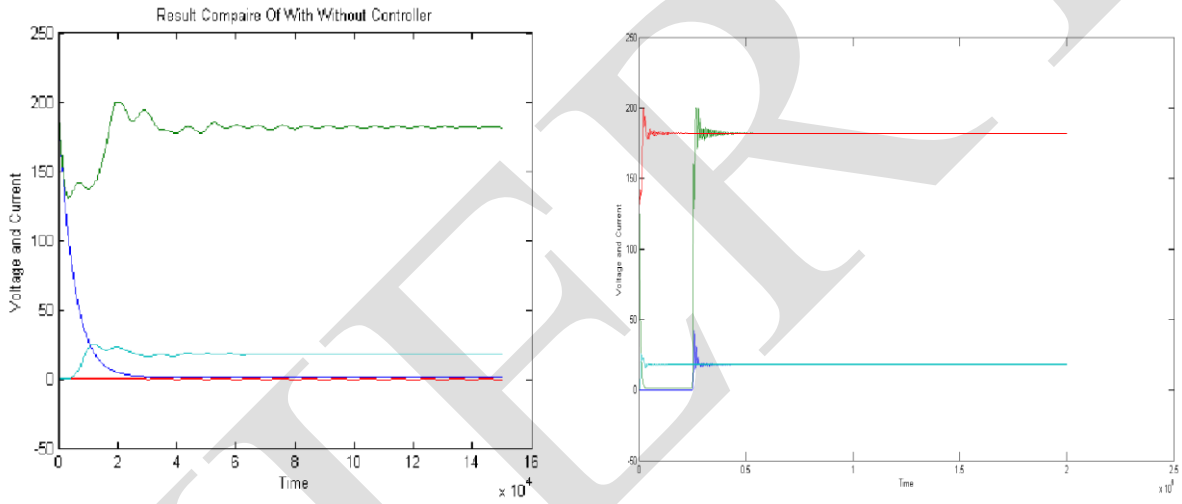

Fig. 15 Waveform Of Two boost-based LFR by using SMC and without SMC

CONCLUSION

An approach is proposed to connect in cascade dc–dc switching converters to obtain high voltage conversion ratios by using the concept of canonical elements in power processing. These canonical elements, named dc transformer, power gyrator, and LFR, have been implemented by means of the SMC technique .the dynamic performance is worse than in the case of dc transformer because of the lower damping factor corresponding to the complex conjugate poles Moreover, compared to the dc-transformer case, the cascaded gyrators do not require the presence of an additional inductor at the output port. The introduction of this element yields also to a fourth order unconditionally stable system but with worse dynamic performance. Finally, the cascade connection of two LFRs results in a second-order unconditionally stable system. In this case, the existence conditions of the sliding-mode regime depend on the load resistance but are less restrictive than in the case of gyrators interconnection The fact that the disturbances that might occur at the output port are not transferred to the input port would allow the implementation of a fast MPPT of the PV generator. Based on this discussion, the cascade connection of boost-based LFRs could be considered as the best option to obtain high voltage conversion ratios with good dynamic performance and good line and load regulation performances. Moreover, as in the case of an individual boost based LFR, the cascaded connection of LFRs could be used to implement electronic functions in energy processing, like PFC in ac–dc applications and MPPT in PV applications [5], where high voltage conversion ratios are needed and the use of high frequency transformers is not a preferred solution

REFERENCES

1) D. Boroyevich, I. Cvetkovic, D. Dong, R. Burgos, F. Wang, and F. Lee, *"Future electronic power distribution systems: A contemplative view," in Proc. IEEE 12th Int. Conf. Optim. Electr. Electron. Equipment, May 2010, pp. 1369–1380.*

2) A. Cellatoglu and K. Balasubramanian, "*Renewable energy resources for residential applications in coastal areas: A modular approach," in Proc.42nd Southeastern Symp. Syst. Theor., Mar. 2010, pp. 340–345.*

3) A. Cid-Pastor, L. Mart´ınez-Salamero, C. Alonso, B. Estibals, J. Alzieu, G. Schweitz, and D.Shmilovitz,"*Analysis and design of power gyrators in sliding- mode operation," IEE Proc. Electr. Power Appl., vol. 152,no.4, pp. 821–826, Jul. 2005*

4) P. Mattavelli, L. Rossetto, G. Spiazzi, and P. Tenti, "*General-purpose sliding-mode controller for DC/DC converter applications," in Proceedings of the IEEE 24th Annual Power Electronics Specialist Conference (PESC '93), pp. 609–615, Seattle, Wash, USA, June 1993. View at Scopus*

5) A. Cid-Pastor, L. Mart´ınez-Salamero, A. El Aroudi, R. Giral, J. Calvente, and R. Leyva, "*Synthesis of loss-free resistors based on sliding-mode control and its applications in power processing," Contr. Eng. Practice,vol. 21, pp. 689–699, May 2013..*

6) L. Mart´ınez-Salamero and A. Cid-Pastor, *"Synthesis of canonical elements for power processing based on sliding-mode control," in Sliding Modes After the First Decade of the 21st Century (Lecture Notes in Control and Information Sciences), vol. 412, L. Fridman, J. Moreno, and R. Iriarte, Eds. Berlin, Germany: Springer, 2012, pp. 517–540.*

7) S. Vighetti, J. P. Ferrieux, and Y. Lembeye, "*Optimization and design of a cascaded dc/dc converter devoted to grid-connected photovoltaic systems," IEEE Trans. Power Electron., vol. 27, no. 4, pp. 2018–2027, Apr. 2012.*